nature catalysis

Article

https://doi.org/10.1038/s41929-025-01402-w

Copper-catalysed enantioconvergent *O*-alkylation of alcohols with racemic α-tertiary haloamides to access enantioenriched hindered dialkyl ethers

Received: 17 October 2024

Accepted: 29 July 2025

Published online: 28 August 2025

Check for updates

Jia-Yong Zhang[1,2,3,5], Ji-Jun Chen[1,2,5], Boming Shen[2,5], Jia-Heng Fang[1,2], Xuan-Yi Du[1,2], Ning-Yuan Yang[1,2], Chang-Jiang Yang[3], Wei-Long Liu[1,2], Fu Liu[2], Zhong-Liang Li[4], Qiang-Shuai Gu[2], Zhe Dong[1,2], Peiyuan Yu[2] ✉ & Xin-Yuan Liu[1,2] ✉

The cross-coupling of bulky electrophiles and nucleophiles to form sterically congested molecules is a challenging issue in modern synthetic chemistry. Among them, chiral hindered dialkyl ethers are one class of valuable motifs, but the catalytic asymmetric synthesis of such motifs from readily available tertiary alcohols and racemic electrophiles remains underexplored. Challenges arise from the steric hindrance of both reactants, the difficulty in enantiodiscriminating the three substituents of tertiary electrophiles and the low nucleophilicity of bulky alcohols. Here we show the copper-catalysed enantioconvergent radical *O*-alkylation of diverse alcohols with racemic α-tertiary haloamides to access enantioenriched hindered dialkyl ethers. Successful realization of this strategy relies on the development of anionic *N*,*N*,*N*-ligands with a side arm to form coordinatively saturated key Cu(III) intermediates, therefore exerting remarkable chemo- and enantioselectivity. The synthetic potential is showcased by the late-stage functionalization and stereodivergent synthesis of four stereoisomers of a product with two stereocentres.

Chiral dialkyl ethers represent a fundamental class of compounds in chemistry. Among them, chiral hindered dialkyl ethers—particularly those bearing bis-tertiary alkyl linkers—are important building blocks and structural elements across natural products and bioactive compounds (Fig. 1a)[1–9]. From a medicinal chemistry perspective, introducing extensive substituents around the ether linkage is likely to impart drug molecules with substantial resistance to undesirable metabolic processes, potentially reducing their rate of degradation in vivo[1,10]. Consequently, the catalytic enantioselective synthesis of such enantioenriched motifs has been an enduring objective in modern chemical and biological research[11–16]. In this regard, the catalytic asymmetric *O*-alkylation of simple alcohols with various alkyl electrophiles provides an efficient method for preparing these compounds[17–32], as alcohols are among the most abundant feedstocks in the chemical industry. Consequently, various catalytic asymmetric methods have been successfully developed, including olefin functionalization[11,17–21], allylic and propargylic substitution reactions[12,13,22,23], carbene insertion into O–H bonds[14,24], cyclopropane ring opening[25,26] and other related transformations[27–32]. Despite these impressive advances, to our best knowledge, no method has yet emerged for the enantioselective synthesis of enantioenriched hindered α,α′-trisubstituted α-stereogenic ethers through direct coupling of the corresponding tertiary (3°) alkyl electrophiles and alcohols, although the racemic reactions have been sporadically reported[33–37]. There are two substantial hurdles: (1) the

A full list of affiliations appears at the end of the paper. ✉e-mail: yupy@sustech.edu.cn; liuxy3@sustech.edu.cn

https://doi.org/10.1038/s41929-025-01402-w

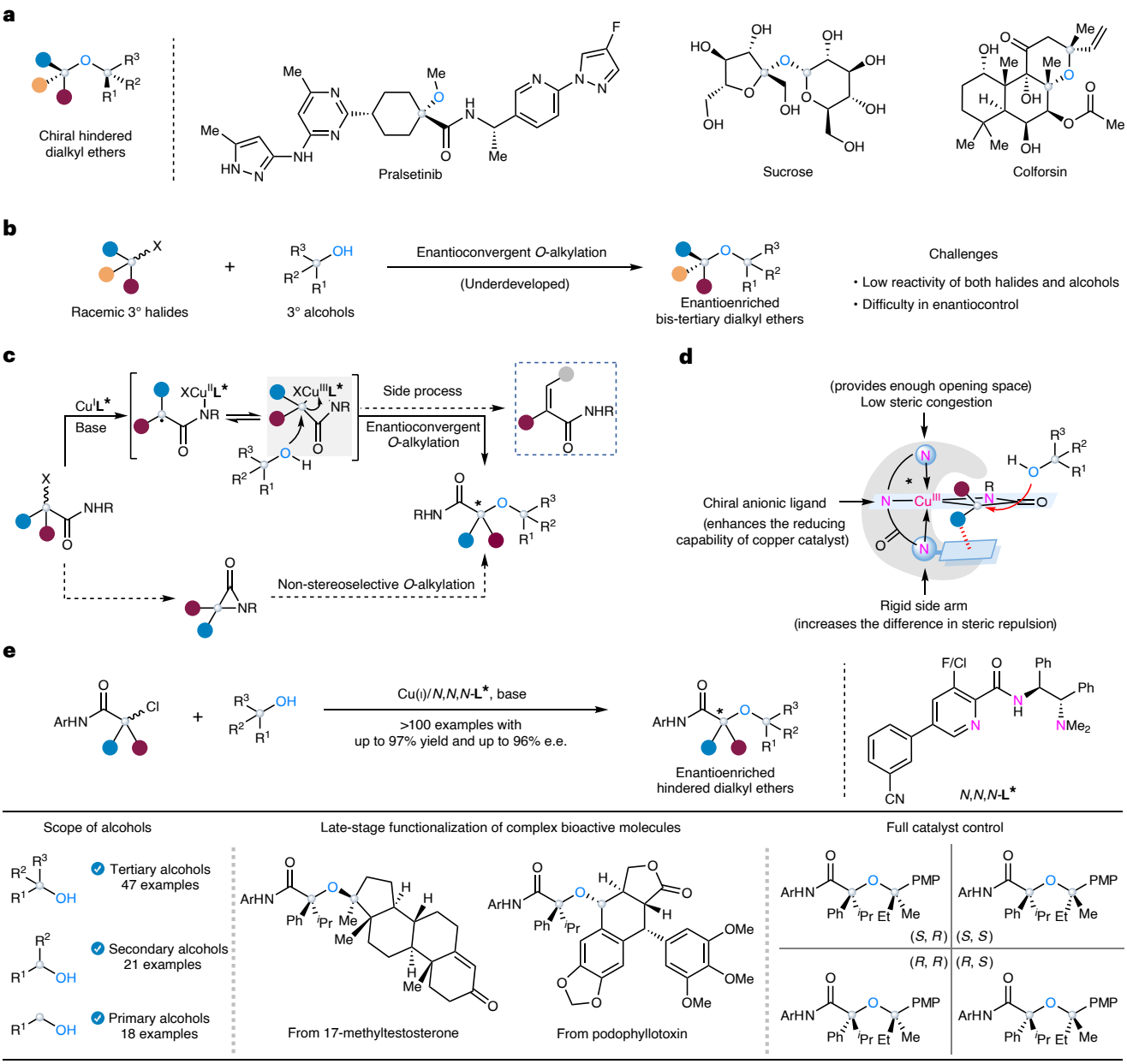

Fig. 1 | Challenges and design of copper-catalysed enantioconvergent *O*-alkylation of tertiary alcohols. a, Examples of chiral hindered dialkyl ethers. **b**, Challenges in the catalytic asymmetric *O*-alkylation of tertiary alcohols with tertiary alkyl electrophiles. **c**, An outer-sphere nucleophilic attack model to provide a new C(sp^3)–O bond formation and allow coupling of the sterically congested tertiary alcohols. **d**, Development of chiral ligands for enantiocontrol coupling of tertiary alcohols with tertiary electrophiles. **e**, This work: copper-catalysed enantioconvergent radical *O*-alkylation of alcohols with α-tertiary haloamides for the synthesis of enantioenriched hindered dialkyl ethers. Ar, 4-cyano-2-methylphenyl; ^{i}Pr, *iso*-propyl; PMP, 4-methoxyphenyl.

steric hindrance of both reactants and the difficulty in enantiodiscriminating the three substituents of tertiary alkyl electrophiles, which would lead to notably low reactivity and enantioselectivity (Fig. 1b); and (2) the relatively weak nucleophilicity of tertiary alcohols (with a nucleophilicity *N* in MeCN of 5.35 for ^{t}BuOH and 6.86 for MeOH)[38] and the strong basicity of the corresponding alkali-metal alkoxides (pK_a in DMSO = 32.2 for ^{t}BuOH and 29.0 for MeOH)[39], which would probably induce competing side reactions.

The traditional Williamson ether synthesis, which couples alcohols and alkyl halides through stereospecific S_N2 substitution, has been the most efficient approach for forging C(sp^3)–O bonds[40–42]. This approach benefits from readily available starting materials and offers high practicality and scalability, making it a cornerstone reaction in both academy and industry. More recently, Fu achieved a notable breakthrough in the enantioconvergent Williamson-type *O*-alkylation of alcohols with racemic α-haloamides to access enantioenriched dialkyl ethers under chiral copper catalysis[43]. Notably, this elegant approach focuses on the coupling of less sterically hindered alcohols and α-secondary haloamides. We have recently found that chiral multidentate anionic ligand/copper catalysts can promote the single-electron reduction of racemic α-haloamides to generate a Cu(III) intermediate, which allows the enantioconvergent *N*-alkylation of amines via an outer-sphere nucleophilic attack model[44,45]. We wondered whether this model could facilitate the enantioconvergent radical *O*-alkylation of sterically hindered alcohols with α-tertiary haloamides to afford enantioenriched hindered dialkyl ethers by overcoming the aforementioned hurdles (Fig. 1b). Nevertheless, two additional challenges still existed. First, non-stereoselective background nucleophilic substitution between

https://doi.org/10.1038/s41929-025-01402-w

Table 1 | Ligand effect in the model reaction and optimal results

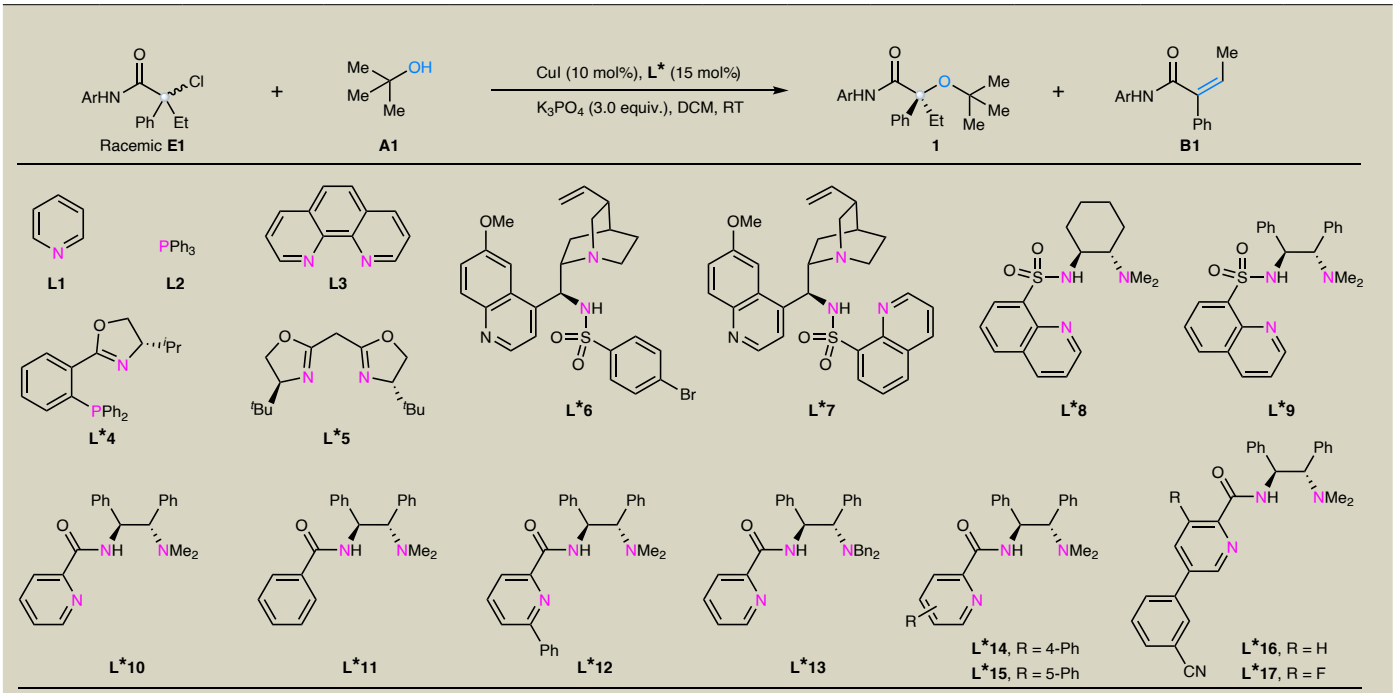

Entry	L*	Conv. of E1 (%)	Yield of 1 (%)	Yield of B1 (%)	e.e. of 1 (%)	Entry	L*	Conv. of E1 (%)	Yield of 1 (%)	Yield of B1 (%)	e.e. of 1 (%)
1[a]	–	19	13	Trace	0	11	**L*9**	37	29	Trace	2
2[b]	–	88	14	70	0	12	**L*10**	99	77	Trace	59
3	**L1**	90	32	48	0	13	**L*11**	81	21	53	10
4	**L2**	97	10	83	0	14	**L*12**	100	10	84	4
5	**L3**	100	22	70	0	15	**L*13**	100	14	83	3
6	**L*4**	100	39	50	14	16	**L*14**	100	74	Trace	60
7	**L*5**	80	26	40	3	17	**L*15**	100	75	Trace	62
8	**L*6**	73	24	38	0	18	**L*16**	100	76	Trace	64
9	**L*7**	38	27	Trace	3	19	**L*17**	100	79	Trace	68
10	**L*8**	48	37	Trace	5	20[c]	**L*17**	100	91	Trace	90

Standard reaction conditions: racemic **E1** (0.05 mmol), *tert*-butanol **A1** (1.5 equiv.), CuI (10 mol%), **L*** (15 mol%) and K_3PO_4 (3.0 equiv.) in dichloromethane (0.50 ml) at room temperature for 48 h under argon. The conversion of **E1** and yields of **1** and **B1** are based on ^{1}H NMR analysis of the crude products using 1,3,5-trimethoxybenzene as an internal standard and the e.e. values are based on chiral high-performance liquid chromatography analysis. [a]Without CuI and **L***. [b]Without **L***. [c]Cu(OTf)·tol$_{1/2}$ (10 mol%), DCE (0.50 ml) at −10 °C for 5 days. Ar, 4-cyano-2-methylphenyl; Bn, benzyl; Conv., conversion; RT, room temperature; ^{t}Bu, *tert*-butyl.

alcohols and α-haloamides easily occurred via the aziridinone intermediate in the presence of an inorganic base[35]. Second, the weak nucleophilicity of bulky alcohols and steric congestion rendered C(sp^3)–O formation from Cu(III) intermediates relatively difficult; thus, many other pathways may compete with the desired process, such as possible β-hydride elimination[46,47] (Fig. 1c). As such, we envisaged that the development of a chiral copper catalyst may help to overcome the difficulties based on three key principles: (1) chiral tridentate anionic ligands would improve the reducing power of the copper catalyst to enable initiation of the radical pathway with high reaction efficiency while circumventing the competitive stereospecific background reaction[35]; (2) the finely tuned ligands could form a coordinatively saturated Cu(III) intermediate with low steric congestion around the metal centre, which could provide enough opening space to accommodate bulky alcohols and suppress side processes; and (3) the incorporation of a rigid side arm into the chiral ligand, remote from the metal centre, could enhance the enantioselectivity by increasing the difference in steric repulsion from substituents at the chiral centre (Fig. 1d).

In this Article, we disclose the successful execution of this strategy through the development of chiral tridentate anionic *N*,*N*,*N*-ligands to realize the enantioconvergent radical *O*-alkylation of alcohols (Fig. 1e). Structure–activity relationship studies indicate that chiral ligands with a remote rigid arm to form two fused five-membered copper catalysts adopting a meridional coordination mode with low steric congestion around the metal centre are important for achieving high chemo- and enantioselectivity. The reaction successfully accommodates different types of alcohols (>80 examples), which are readily available building blocks or drug molecules. In particular, the current approach directly couples the most challenging α-tertiary haloamides and tertiary alcohols for the synthesis of enantioenriched hindered ethers, allowing easy accommodation of both sterically congested coupling reagents and providing an important complementary approach to the existing chiral C(sp^3)–O formation protocols[17–32,35,43]. More importantly, the reaction could provide all four possible stereoisomers of hindered dialkyl ethers with two chiral centres with high catalyst-controlled stereoselectivity.

Results

Reaction development

Given the lack of reports on the synthesis of enantioenriched hindered ethers via the cross-coupling of tertiary electrophiles with alcohols, we

https://doi.org/10.1038/s41929-025-01402-w

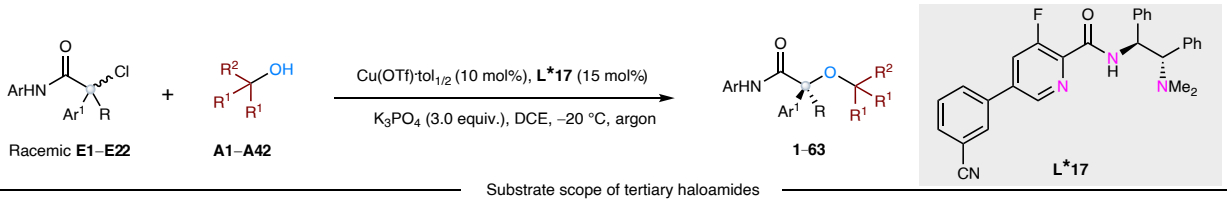

Substrate scope of tertiary haloamides

Scope of Ar^1 in alkyl chlorides

(1–10)

1, 88%, 90% e.e.[a]; 2, 57%, 91% e.e.; 3, 54%, 90% e.e.; 4, 59%, 91% e.e.; 5, 66%, 91% e.e.

6, 54%, 87% e.e.[b]; 7, 75%, 83% e.e.; 8, 59%, 80% e.e.[b,c]; 9, 68%, 91% e.e.; 10, 64%, 90% e.e.

Scope of R in alkyl chlorides

(11–22)

11, 51%, 87% e.e.[b]; 12, 45%, 88% e.e.[b]; 13, 55%, 84% e.e.; 14, 57%, 87% e.e.; 15, 60%, 83% e.e.; 16, 72%, 96% e.e.[a]

17, 62%, 90% e.e.[a]; 18, 85%, 90% e.e.[a]; 19, 74%, 90% e.e.[a]; 20, 78%, 95% e.e.[a]; 21, 58%, 87% e.e.; 22, 62%, 49% e.e.[a,d]

Substrate scope of tertiary alcohols[e]

23, 76%, 90% e.e.; 24, 62%, 90% e.e.; 25, 68%, 90% e.e.; 26, 82%, 95% e.e.[f]; 27, 56%, 90% e.e.; 28, 62%, 90% e.e.; 29, 71%, 95% e.e.[f]

30, 53%, 90% e.e.; X-ray structure of 30; 31, 64%, 95% e.e.[f]; 32, 63%, 95% e.e.[f]; 33, 68%, 95% e.e.[f]; 34, 59%, 92% e.e.[f]; 35, 72%, 94% e.e.[f]

36, 67%, 94% e.e.[f]; 37, 42%, 94% e.e.[f]; 38, 57%, 93% e.e.[f]; 39, 69%, 94% e.e.[f]; 40, 64%, 95% e.e.[f]; 41, 78%, 92% e.e.; 42, 57%, 90% e.e.

43, 65%, 91% e.e.; 44, 57%, 94% e.e.[f]; 45, 51%, 90% e.e.; 46, 58%, 90% e.e.; 47, 63%, 90% e.e.; 48, 57%, 95% e.e.[f]; 49, 42%, 90% e.e.

50, 74%, 91% e.e.; 51, 81%, 90% e.e.; 52, 56%, 91% e.e.; 53, 73%, 91% e.e.; 54, 61%, 91% e.e.[f]; 55, 54%, 95% e.e.[f]; 56, 64%, 90% e.e.

57, 62%, 95% e.e.[f]; 58, 48%, 87% e.e.[f]; 59, 46%, 90% e.e.; 60, 56%, 95% e.e.[f]; 61, 61%, 94% e.e.[f]; 62, 67%, 95% e.e.[f]; 63, 91%, 82% e.e.[a]

Fig. 2 | Substrate scope for α-tertiary haloamides and tertiary alcohols. Standard reaction conditions: racemic α-tertiary haloamides (0.20 mmol), tertiary alcohol (1.5 equiv.), Cu(OTf)·$tol_{1/2}$ (10 mol%), **L*17** (15 mol%) and K_3PO_4 (3.0 equiv.) in DCE (2.0 ml) at −20 °C for 7 days under argon. Isolated yields are shown, followed by e.e. values based on chiral high-performance liquid chromatography analysis. [a]At −10 °C for 5 days. [b]In $PhCF_3$. [c]At −10 °C. [d]Alkyl bromide was used. [e]**E1** (Ar^1 = Ph; R = Et) was used. [f]**E16** (Ar^1 = Ph; R = ^{i}Pr) was used at −10 °C for 5 days. Ar, 4-cyano-2-methylphenyl; Boc, *tert*-butyloxycarbonyl; Bz, benzoyl; ^{n}Bu, *n*-butyl; ^{n}Pr, *n*-propyl; TBS, *tert*-butyldimethylsilyl.

https://doi.org/10.1038/s41929-025-01402-w

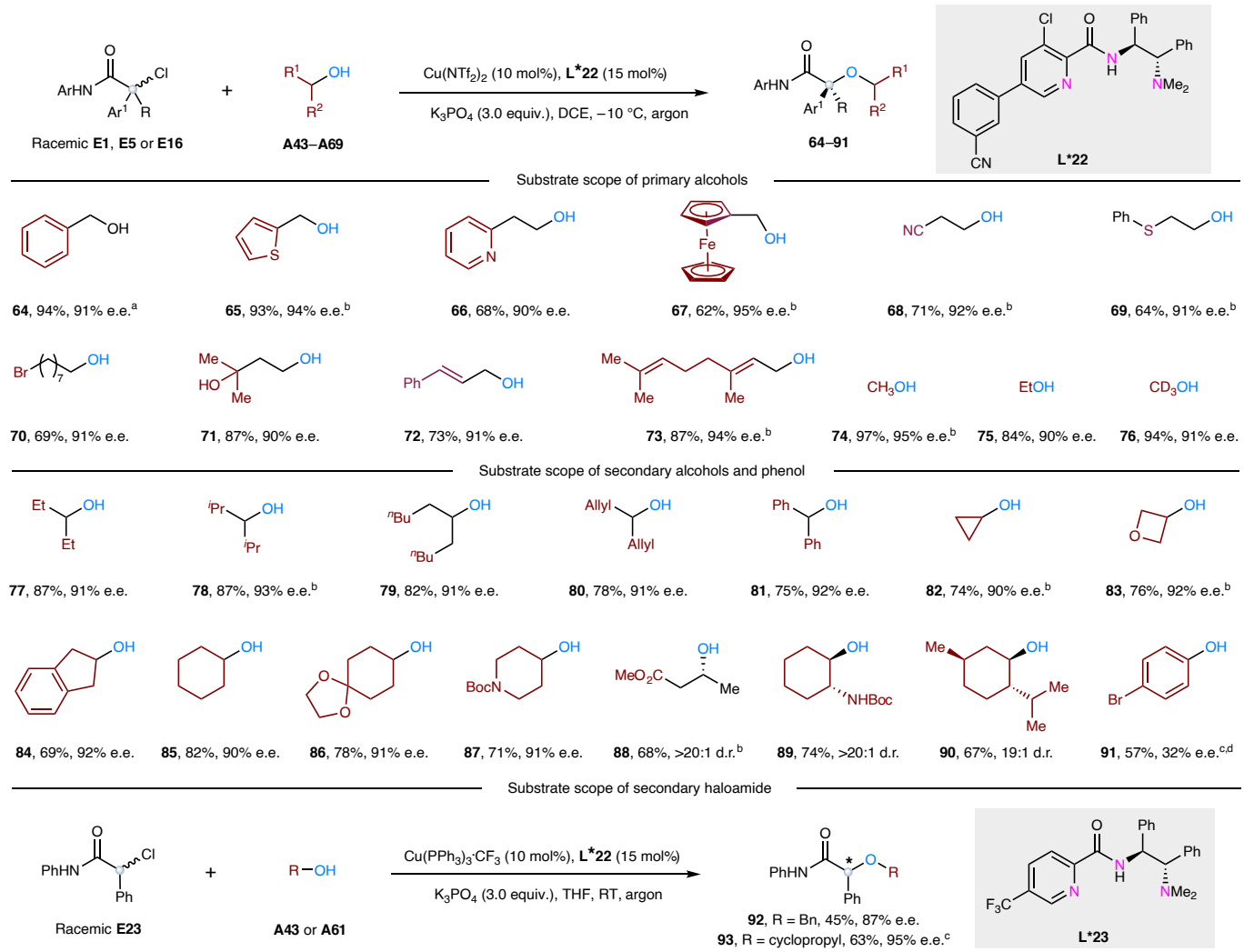

Fig. 3 | Substrate scope for primary and secondary alcohols or α-secondary haloamides. Standard reaction conditions: racemic **E5** (Ar^1 = 3-$MeOC_6H_4$; R = Et; 0.20 mmol), primary or secondary alcohol (1.5 equiv.), $Cu(NTf_2)_2$ (10 mol%), **L*22** (15 mol%) and K_3PO_4 (3.0 equiv.) in DCE (2.0 ml) at −10 °C for 5 days under argon. Isolated yields are shown, followed by e.e. values based on chiral high-performance liquid chromatography analysis or d.r. values based on crude ^{1}H NMR analysis. [a]**E1** was used. [b]**E16** was used. [c]**L*23** was used. [d]**E1** (0.20 mmol) and 4-bromophenol (1.2 equiv.) in *p*-xylene (2.0 ml) at room temperature for 3 days. Ar, 4-cyano-2-methylphenyl; d.r., diastereomeric ratio; THF, tetrahydrofuran; RT, room temperature.

first sought to identify a simple model system for exploring the catalyst and ligand structure–activity relationship. Accordingly, we investigated the most challenging enantioconvergent *O*-alkylation reaction of *tert*-butanol **A1** with racemic α-tertiary haloamide (±)-**E1** based on our previous reports[44,45] (Table 1 and Supplementary Tables 1–5). Indeed, the addition of K_3PO_4 without copper catalyst in dichloromethane gave the *O*-alkylation product **1**, presumably via stereospecific nucleophilic substitution[35] (entry 1). When the catalyst CuI (10 mol%) was added, the conversion of (±)-**E1** was greatly improved (entry 2). However, the reaction afforded a large amount of side product **B1** (Supplementary Figs. 4 and 5). We next sought to increase the chemoselectivity through the screening of chiral ligands. Unfortunately, mono- and bidentate ligands such as **L1**–**L*4**, bisoxazoline **L*5** for Fu's enantioconvergent *O*-alkylation[43] and anionic sulfonamide *N*,*N*-ligand **L*6** for our enantioconvergent *N*-alkylation[44] still provided a large amount of side product **B1** (entries 3–8). We speculated that **B1** might be derived from the intramolecular β-hydride elimination of the thus-generated Cu(III) intermediate with a vacant coordinating site[48]. To promote the desired pathway, we utilized chiral tridentate ligands to form a putative coordinatively saturated Cu catalyst[48], which would lead to inhibition of the possible β-hydride elimination. We found that a series of tridentate anionic sulfonamide ligands **L*7**–**L*9** resulted in a substantial decrease of **B1**. However, low reaction efficiencies and enantioselectivities were still observed (entries 9–11). X-ray structural analysis of complex **C1** derived from copper and **L*8** revealed that the tridentate *N*,*N*,*N*-ligand coordinates to the Cu centre in a sterically bulky facial coordination mode, influenced by the rigid quinoline-8-sulfonamide, which probably affected the reaction efficiency (Fig. 6a).

We then decided to investigate the use of alternative chiral tridentate anionic *N*,*N*,*N*-ligands to provide sufficient space to accommodate the bulky alcohols. To our delight, the use of anionic amide ligand **L*10** bearing a pyridine ring greatly enhanced both the yield and enantioselectivity of **1** (entry 12). Notably, **L*10** coordinates with copper in a meridional configuration to form a stable fused five-membered copper complex **C2** with low steric congestion around the metal centre (Fig. 6a and Supplementary Fig. 10), in contrast with the bulky facial coordination observed in complex **C1**. To further demonstrate the role of the coordinating pyridine, we replaced it with a phenyl ring (**L*11**) or *ortho*-substituted pyridyl ring (**L*12**) and found greatly diminished chemoselectivity (entries 13 and 14). The use of ligand **L*13** with a bulkier *N*,*N*-dibenzyl amino group also resulted in decreased chemoselectivity, highlighting the negative impact of steric hindrance in the coordinating

https://doi.org/10.1038/s41929-025-01402-w

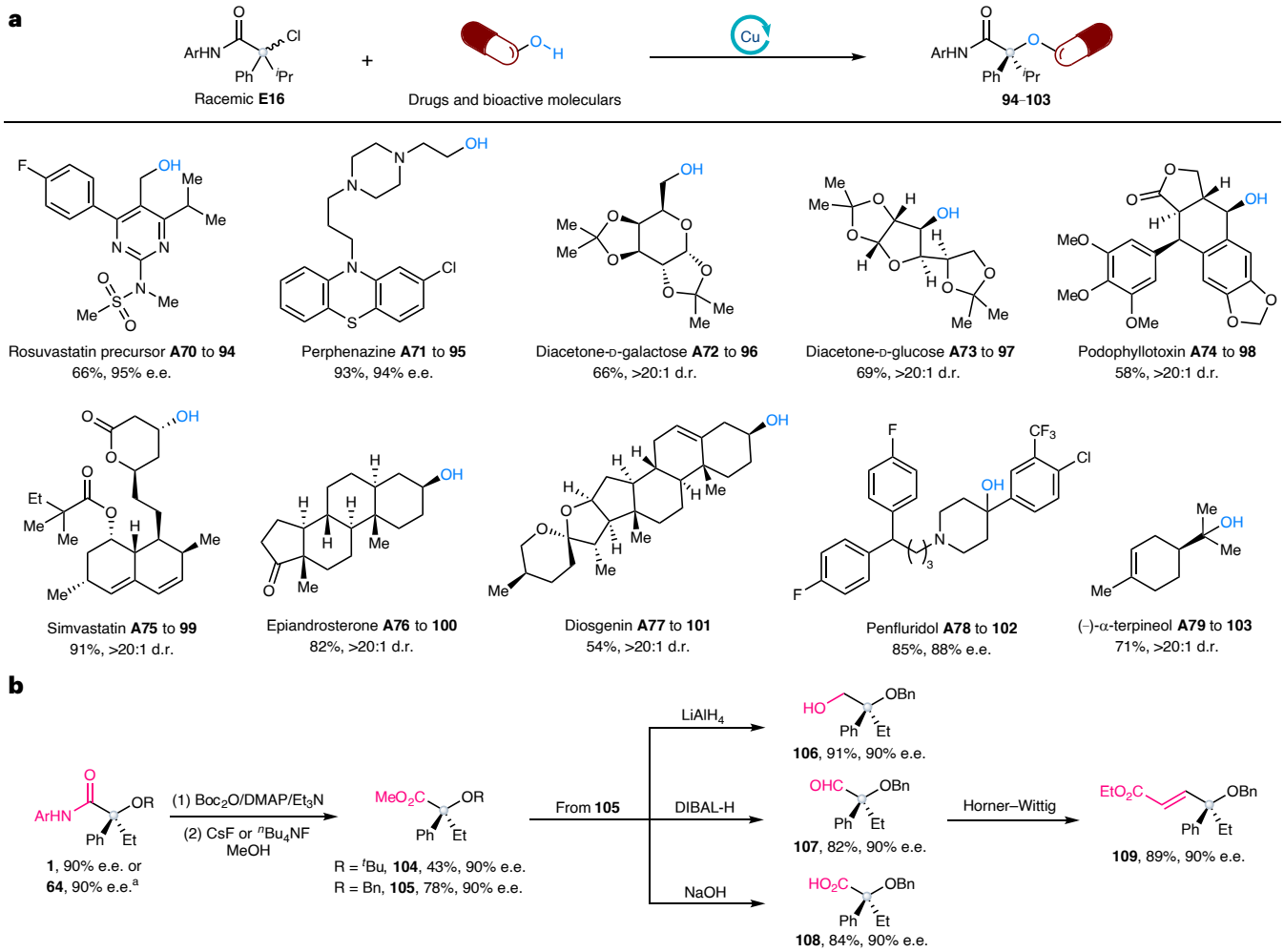

Fig. 4 | Synthetic utility. a, Late-stage enantioconvergent *O*-alkylation of drugs and bioactive molecules with racemic α-tertiary haloamide. **b**, Practical and expedient transformation of enantioenriched hindered dialkyl ethers to other valuable chiral building blocks. [a]A gram-scale (2.50-mmol) reaction was performed to afford **64** with good yield and e.e. Ar, 4-cyano-2-methylphenyl; DIBAL-H, diisobutylaluminum hydride; DMAP, 4-dimethylaminopyridine.

centre (entry 15). These results underscore the importance of finely tuned chiral tridentate amide *N*,*N*,*N*-ligands in forming a coordinatively saturated Cu(III) intermediate with low steric congestion, which is crucial for tuning the chemoselectivity and enhancing the reactivity of the reaction. It is noteworthy that installation of a side arm on the pyridine ring (**L*14**–**L*17**) further increased the enantioselectivity, indicating that crucial stereodiscriminating interactions far from the copper centre are necessary[49] (entries 16–19). The investigation of other parameters, including copper catalysts, reaction temperature and solvents with the ligand **L*17** (Supplementary Tables 1–5) led to the following optimal conditions: the reaction of racemic **E1** and **A1** using catalytic amounts of Cu(OTf)·tol$_{1/2}$ and **L*17**, with K_3PO_4 as the base in 1,2-dichloroethane (DCE) at −10 °C gave rise to **1** in 91% yield with 90% e.e. (Table 1, entry 20).

Substrate scope

Having established the optimal reaction conditions, we proceeded to assess the reaction generality. Concerning the scope of α-tertiary haloamides (Fig. 2), a range of α-monosubstituted phenyl rings bearing diverse functional groups—regardless of their electronic nature at the *meta* and *para* positions—as well as disubstituted phenyl rings were tolerated to deliver **1**–**10** with 80–91% e.e. As for the α-alkyl substitution pattern, substrates bearing linear aliphatic chains with either no functional group or terminal olefin, phenyl and ether groups, as well as more hindered acyclic and cyclic secondary alkyl groups, were well accommodated to deliver **11**–**21** in 45–85% yields with 83–96% e.e. In addition, by utilizing the corresponding α,α-dialkyl-substituted electrophile as the substrate, the desired product **22** could be obtained with promising enantioselectivity, and this is currently undergoing further optimization in our laboratory.

We next evaluated the scope of bulky tertiary alcohols (Fig. 2). A broad series of acyclic trialkyl-substituted alcohols could readily participate in this reaction to afford **23**–**42** in 42–82% yields with 90–95% e.e. Different kinds of functional groups, such as trifluoromethyl (**31**), methoxy (**32**) and tertiary amino (**38**), as well as radical-sensitive terminal olefins (**39**–**41**) and alkyne (**42**), were all compatible with the reaction conditions. Particularly noteworthy is that the tertiary alcohols bearing sensitive functional groups under acidic or basic conditions, such as benzoyl- and *tert*-butyldimethylsilyl-protected alcohols (**33** and **34**), ester (**36**), Boc-protected amine (**37**) and free alcohol (**35**), were also allowed. Acyclic tertiary alcohols containing different types of α-substituted (hetero)aryl rings, including mono-/disubstituted phenyl rings (**43**–**45**), a naphthyl ring (**46**), furan (**47**), thiophene (**48**) and indole (**49**), were viable substrates. Additionally, cyclic tertiary alcohols bearing different ring sizes (four- to 12-membered rings; **50**–**57**), as well as medicinally relevant saturated heterocycles such as oxetane (**58**), azetidine (**59**), tetrahydro-2*H*-pyran (**60**) and piperidine (**61**), were appropriate reaction partners. Importantly, 1-adamantanol (**62**) and trimethylsilanol (**63**) could be alkylated with high efficiency and good enantioselectivity.

https://doi.org/10.1038/s41929-025-01402-w

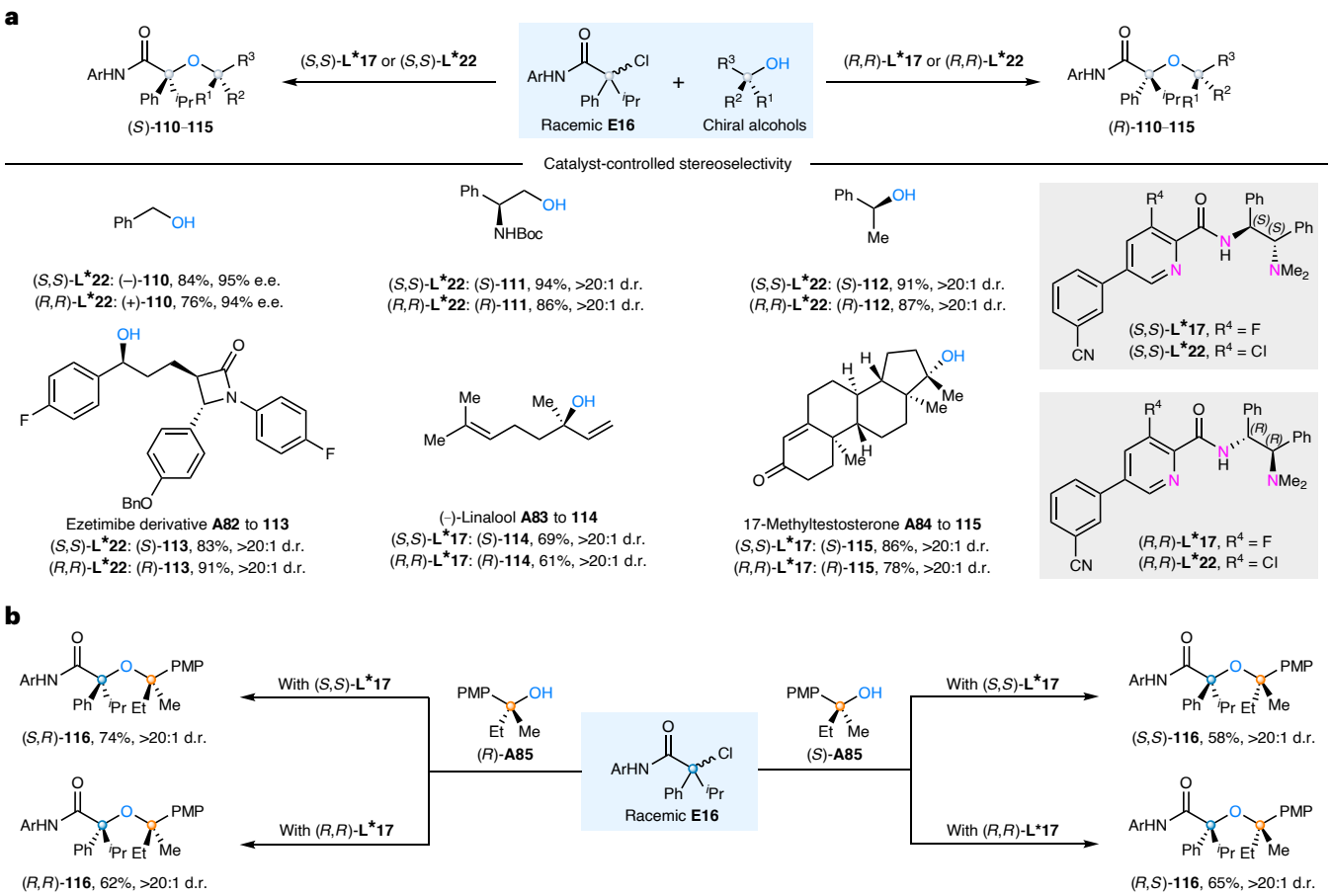

Fig. 5 | Catalyst-controlled stereoselective and stereodivergent synthesis. **a**, Stereoselective synthesis of enantioenriched hindered dialkyl ethers via catalyst-controlled *O*-alkylation of alcohols with racemic α-tertiary haloamide. **b**, Stereodivergent synthesis of all four stereoisomers of sterically hindered dialkyl ether via catalyst-controlled *O*-alkylation of chiral tertiary alcohols. Ar, 4-cyano-2-methylphenyl; PMP, 4-methoxyphenyl.

To further enhance the synthetic application, we investigated the asymmetric *O*-alkylation reaction of primary and secondary alcohols. Ligand **L*17** only showed moderate reaction efficiency in the *O*-alkylation of benzyl alcohol **A43** (77% yield for **64**; Supplementary Table 6). Further modification of the *N*,*N*,*N*-ligands and reaction screening led us to identify the optimal conditions for the asymmetric *O*-alkylation of primary and secondary alcohols as follows: the reaction of racemic **E1** and **A43** using a catalytic amount of $Cu(NTf_2)_2$ and **L*22** in the presence of K_3PO_4 in DCE at −10 °C afforded **64** in 94% yield with 91% e.e. (Supplementary Tables 6 and 7). With regard to the substrate scope (Fig. 3), a broad array of primary and secondary alcohols bearing many functional groups at different positions could be utilized as substrates in this reaction to afford **64**–**90** in 62–97% yields with 90–95% e.e. Notably, this catalytic system provided remarkably high efficiency and excellent enantioselectivity for the *O*-alkylation of bulk industrial feedstocks such as methanol (**74**) and ethanol (**75**), as well as deuterated methanol (**76**). Interestingly, α-chiral alcohols were also appropriate substrates to give the desired products **88**–**90** with high efficiency and excellent diastereoselectivity. In addition, the *O*-alkylation of 4-bromophenol with α-tertiary haloamide (±)-**E1** also delivered product **91**, which is presently under further optimization in our laboratory. We further found that α-secondary haloamide (±)-**E23** was also suitable for the *O*-alkylation reaction with primary and secondary alcohols to deliver products **92** and **93** with high efficiency and enantioselectivity. X-ray crystallographic analysis confirmed the *S* configuration of **30**, **56**, **64** and **81** (Fig. 2 and Supplementary Figs. 6–9). The configurations of the other compounds were assigned accordingly by analogy.

Synthetic utility

Alcohols are also prevailing motifs in marketed small-molecule pharmaceutical agents and preclinical candidates[50]. To this end, the excellent functional group compatibility of this process offers an opportunity for late-stage modifications of drug molecules or biomolecules with reactive functionalities, streamlining the diversification of highly functional drug leads. For example, more than ten drug molecules (rosuvastatin precursor, perphenazine, simvastatin, epiandrosterone and penfluridol) or biomolecules (diacetone-D-galactose, diacetone-D-glucose, podophyllotoxin, diosgenin and (−)-α-terpineol) could be installed in the α-position of the carbonyl moiety while introducing a chiral centre with other functional groups untouched (Fig. 4a). This process would deliver complex hindered dialkyl ethers **94**–**103** in good yields with excellent enantioselectivity or diastereoselectivity, demonstrating the potential utility of this strategy in early-stage drug discovery. On the gram scale, the reaction performed well, delivering product **64** with consistent yield and enantioselectivity. Notably, the presence of a readily transformable carboxamide moiety of products can further enhance the synthetic potential of this strategy, which can be exploited to generate other valuable enantioenriched building blocks (Fig. 4b). For instance, we converted the carboxamide moiety of **1** and **64** to an ester group via alcoholysis, providing **104** and **105** with acceptable yields. Subsequently, **105** underwent reduction or hydrolysis to give alcohol **106**, aldehyde **107** and carboxylic acid **108**, respectively. More importantly, the aldehyde moiety of **107** was transformed to give the carbon chain-lengthened alkene **109** via the Horner–Wittig reaction. Notably, no notable erosion of e.e. was detected during the course of these transformations.

https://doi.org/10.1038/s41929-025-01402-w

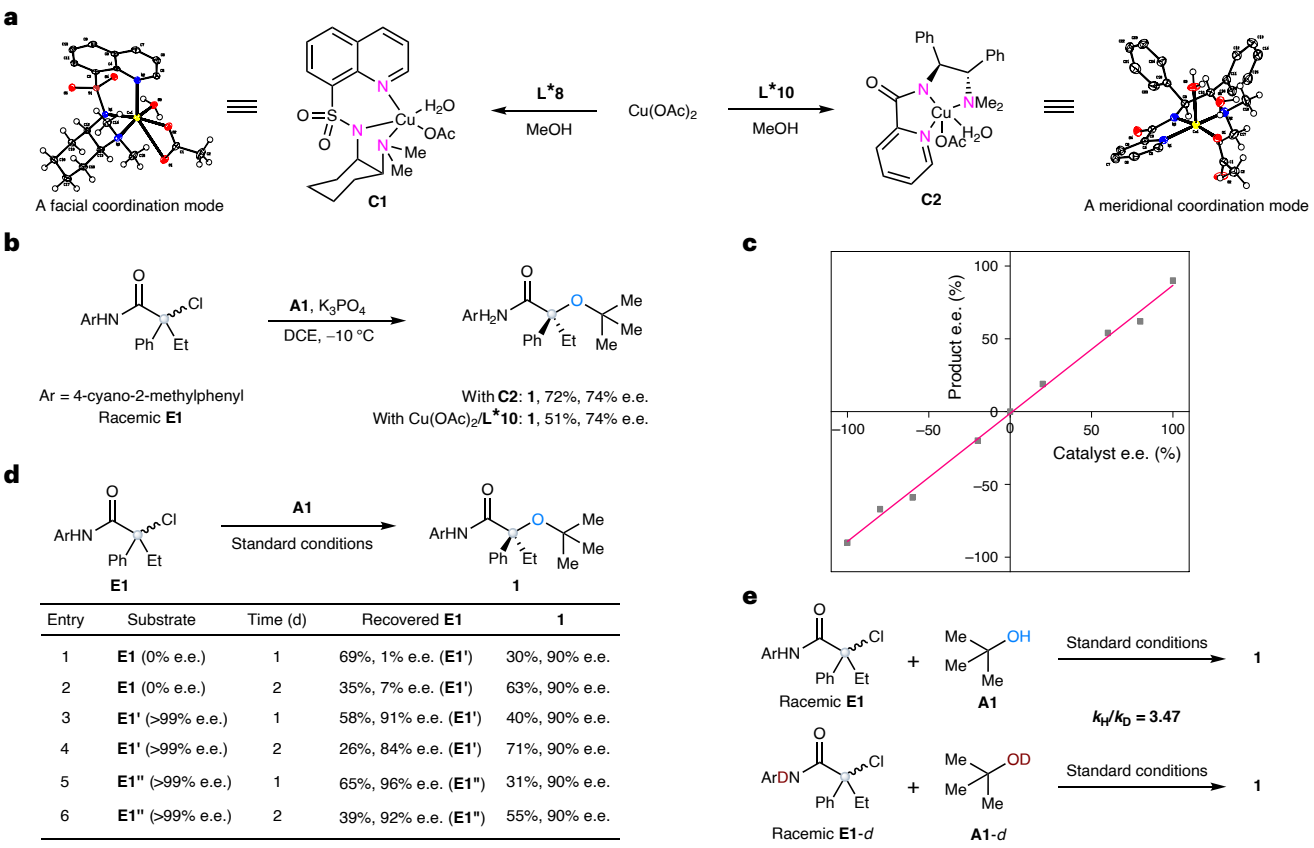

Entry	Substrate	Time (d)	Recovered **E1**	**1**
1	**E1** (0% e.e.)	1	69%, 1% e.e. (**E1'**)	30%, 90% e.e.
2	**E1** (0% e.e.)	2	35%, 7% e.e. (**E1'**)	63%, 90% e.e.
3	**E1'** (>99% e.e.)	1	58%, 91% e.e. (**E1'**)	40%, 90% e.e.
4	**E1'** (>99% e.e.)	2	26%, 84% e.e. (**E1'**)	71%, 90% e.e.
5	**E1"** (>99% e.e.)	1	65%, 96% e.e. (**E1"**)	31%, 90% e.e.
6	**E1"** (>99% e.e.)	2	39%, 92% e.e. (**E1"**)	55%, 90% e.e.

Fig. 6 | Mechanistic discussion. a, Left, synthesis of the copper(II) complex **C1** and an X-ray structure showing a facial coordination mode. Right, synthesis of the copper(II) complex **C2** and an X-ray structure showing a meridional coordination mode. **b**, Complex **C2** exhibited comparable catalytic activity to that generated in situ from $Cu(OAc)_2$ and **L*10**. **c**, The observed linear relationship between the enantiopurities of products and ligands strongly indicated a 1:1 ratio of copper to ligand in the enantio-determining step. **d**, Although there was partial racemization of enantioenriched **E1** or slight enantioenrichment of (±)-**E1** upon recovery, the nearly constant product enantiopurity indicated a uniform enantio-determining transition state throughout the reaction. The two enantiomers of **E1** are denoted as **E1'** and **E1"**. **e**, The measured intermolecular kinetic isotope effect data (3.47) for substrates suggested that the deprotonation process might be involved in the rate-determining step of the *O*-alkylation with tertiary alcohols.

Based on the proposed outer-sphere nucleophilic attack mechanism, we envisioned that the present catalytic system would achieve high enantioselectivity through full catalyst control, irrespective of the pre-existing stereocentres in chiral substrates[44,45]. Indeed, we were delighted to find that the direct *O*-alkylation of diverse chiral alcohols gave the desired products (*S*)-**111**–(*S*)-**115** with high diastereoselectivity in the presence of **L*17** or **L*22** (Fig. 5a). Replacing these ligands with their enantiomers generated the other diastereomers of (*R*)-**111**–(*R*)-**115** with high diastereoselectivity as well. It is well known that the complete set of all stereoisomers of a product with multiple stereocentres via a stereodivergent process is of paramount importance in pharmaceutical applications to evaluate the biological activity of each stereoisomer[51,52]. Encouraged by the above success and given the easy availability of both enantiomers of chiral alcohols, we surmised that such an approach would enable the synthesis of all possible diastereoisomers and enantiomers. To our delight, we found that the *O*-alkylation of chiral alcohols (*R*)-**A85**/(*S*)-**A85** with ligands (*R*,*R*)-**L*17**/(*S*,*S*)-**L*17** could readily provide each of the four stereoisomers of hindered α,α′-trisubstituted α-stereogenic ether **116** with high catalyst-controlled stereoselectivity (Fig. 5b). These results clearly demonstrate that this approach would have broad synthetic applications for achieving stereochemical diversity in library design.

Mechanistic considerations

A control experiment with a catalytic amount of the Cu(II)**L*10** complex **C2** could afford **1** with 72% yield and 74% e.e., comparable to that of the standard reaction conditions (Fig. 6b and Supplementary Table 4). Furthermore, the enantiopurities of the products showed a linear correlation with those of the corresponding ligands (Fig. 6c). These findings provide evidence that a mononuclear copper species coordinated to a chiral *N*,*N*,*N*-ligand was probably the active catalyst in this process. Furthermore, the e.e. of product **1** remained almost constant with the two enantiomers of **E1** (**E1'** and **E1"**) and the racemic substrate (±)-**E1** at different time intervals (Fig. 6d). These results indicated that the whole process probably involved a uniform mechanism for both enantiomers of alkyl halides. Partial racemization of the two recovered enantiomers **E1** or slight enantioenrichment of recovered (±)-**E1** was observed without alcohol **A1** (Fig. 6d; see also Supplementary Fig. 1). These results suggested that the Cu/*N*,*N*,*N*-ligand catalyst could undergo a reversible halogen-atom transfer without nucleophiles, which was further supported by density functional theory (DFT) studies (Fig. 7a). More importantly, kinetic experiments with deuterated and non-deuterated alcohol **A1** provided an intermolecular kinetic isotope effect value of 3.47 (Fig. 6e). Further kinetic experiments were carried out for the *O*-alkylation reaction of *tert*-butanol **A1** with α-tertiary haloamide **E1**. This reaction showed a first-order dependence on tertiary alcohol **A1**, whereas it followed the trend of a zero-order dependence on **E1** (Supplementary Figs. 2 and 3). These results indicated that tertiary alcohols probably underwent concerted nucleophilic attack/deprotonation in the key C(sp^3)–O bond formation step and this step might be the rate-determining step, which was also consistent with the DFT calculations (Fig. 7a).

https://doi.org/10.1038/s41929-025-01402-w

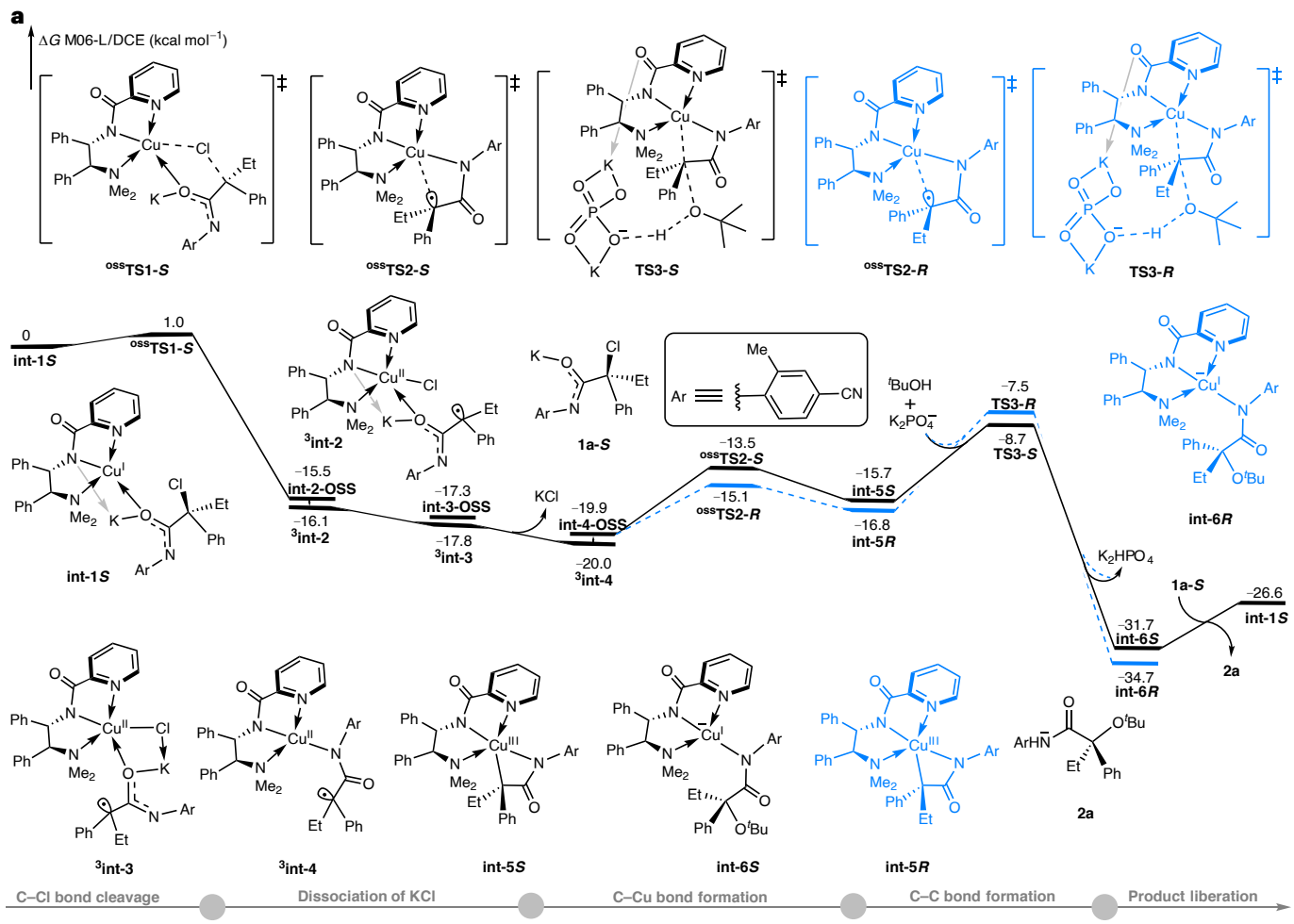

TS3-*S*	(0 kcal mol^{-1})	TS3-*R*	(1.2 kcal mol^{-1})
Type	$\nabla^2\rho$	Type	$\nabla^2\rho$
(1) C–H ··· π	0.489	(1) π ··· π	0.182
(2) C–H ··· π	0.240	———	———
(3) C–H ··· π	0.126	———	———
(4) C–H ··· π	0.288	———	———
(5) C–H ··· π	0.278	———	———

Fig. 7 | Model DFT studies on the operative catalytic cycle and enantioselectivity control. a, Free-energy profile for the copper-catalysed enantioconvergent *O*-alkylation of *tert*-butanol **A1** with **E1** using the truncated model ligand **L*10**. **b**, Atoms-in-molecules analyses of the transition states **TS3-*S*** and **TS3-*R*** and a summary of the Laplacian electron density values ($\nabla^2\rho$). **c**, Optimized structures of the enantioselectivity-determining C(sp^3)–O bond formation transition states **TS4-*S*** and **TS4-*R*** using the optimal ligand **L*17** with the phenyl side arm, as well as **TS3-*S*** and **TS3-*R*** using the truncated model ligand **L*10** without the phenyl side arm. The energy values are given in kcal mol^{-1} and represent the relative free energies calculated at the M06-L/6-311+G(d,p)-SDD-SMD(DCE)//B3LYP-D3(BJ)/6-31G(d)-SDD level of theory. The distances are given in Ångstrom.

To further shed light on the reaction mechanism, DFT calculations were performed on the reaction of **E1** and **A1** with ligand **L*10** (Fig. 7a and Supplementary Figs. 20–25). As shown in Fig. 7a, the copper(I) complex **int-1*S*** derived from the *S*-configured **E1** was chosen as the starting point for the computed free-energy profiles and was more stable than the N- and Cl-bound complexes (Supplementary Fig. 20). Homolytic cleavage of the C–Cl bond in **int-1*S*** proceeded through an open-shell singlet (OSS) chlorine atom transfer transition state (^{OSS}**TS1**) with a very low energy barrier of 1.0 kcal mol^{-1} to generate an OSS-state Cu(II) intermediate **int-2-OSS**, which released 15.5 kcal mol^{-1} free energy. Moreover, we also performed additional DFT calculations for the chlorine atom transfer process to generate **int-2-OSS** for the *R*-configured **E1**, which showed a similar result to that of the *S*-configured **E1** (Supplementary Fig. 21). Intermediate **int-2** had both triplet and OSS states, with the triplet state ^{3}**int-2** being more stable than the latter one (**int-2-OSS**) by 0.6 kcal mol^{-1} in free energy. Subsequently, the radical-potassium fragment detached from the ligand amide group and coordinated to the copper-bound Cl, affording a more stable triplet Cu(II) intermediate ^{3}**int-3**. Intermediate ^{3}**int-3** could then release potassium chloride to afford an *N*-bound triplet Cu(II) intermediate ^{3}**int-4**. The triplet intermediate ^{3}**int-4** then interconverted with intermediate **int-4-OSS**, followed by the subsequent intramolecular single-electron oxidative addition of a tertiary carbon radical to the Cu(II) centre via an OSS transition state ^{OSS}**TS2-*S*** with an energy barrier of 6.5 kcal mol^{-1}. This process generated a Cu(III) intermediate **int-5*S***, which was endergonic by 4.3 kcal mol^{-1}. The intermolecular nucleophilic substitution of alcohol **A1** to intermediate **int-5*S*** assisted by the $K_2PO_4^-$ anion then proceeded via a concerted transition state **TS3-*S*** with an energy barrier of 7.0 kcal mol^{-1} to generate a quaternary stereogenic centre in the thermodynamically stable *N*-bound intermediate **int-6*S*** (Supplementary Fig. 22). Another possibility to form the potassium form **int-6*S*-K** was less likely due to its highly endergonic nature (Supplementary Fig. 23). Finally, the ligand exchange of intermediate **int-6*S*** took place to liberate **2a** and regenerated intermediate **int-1*S***. Notably, the computational results revealed that the intermolecular nucleophilic substitution step was the enantio- and rate-determining step for this reaction, consistent with the kinetic studies (Supplementary Figs. 2 and 3).

Regarding the stereochemistry, intramolecular single-electron oxidative addition via transition state ^{OSS}**TS2-*R*** reversibly generated a Cu(III) intermediate **int-5*R***, the precursor of the *R*-configured product. The subsequent intermolecular nucleophilic substitution via **TS3-*R*** had an activation free energy of 9.3 kcal mol^{-1}. The relative free energy of **TS3-*R*** was 1.2 kcal mol^{-1} higher than that of **TS3-*S***, indicating that formation of the *R*-configured product was unfavourable (Fig. 7a). Based on the relative energies of **TS3-*S*** and **TS3-*R***, the calculated e.e. value was 82%, which slightly overestimated the corresponding experimental result (74% e.e.; Supplementary Table 4).

To further investigate the origin of stereoselectivity, we carried out quantitative Bader's atoms-in-molecules analyses for **TS3-*S*** and **TS3-*R***. The strength of the non-covalent interactions could be quantitatively measured via the values of Laplacian of electron densities ($\nabla^2\rho$). As depicted in Fig. 7b, five C–H···π (2.40, 2.71, 2.97, 2.62 and 2.66 Å) interactions were found in **TS3-*S***, whereas only one π···π (3.33 Å) interaction existed in **TS3-*R***. The non-covalent interactions in **TS3-*S*** were probably stronger than those observed in **TS3-*R***. Therefore, these weak interactions contributed to the stabilization of transition state **TS3-*S*** and were the most important factors for achieving high enantioselectivity. Of note, the installation of a side arm at the *meta*-position on the pyridyl group in ligand **L*10** could increase the enantioselectivity (from 74 to 90% e.e.; Supplementary Table 4). To elucidate the origin of the side-arm effects on the enantioenhancement, we studied the corresponding enantio-determining transition states **TS4-*S*** and **TS4-*R***. The optimized geometries of transition states **TS4-*S*** and **TS4-*R*** were then compared (Fig. 7c). In transition state **TS4-*R***, the introduction of a phenyl side arm could lead to additional steric repulsion between the phenyl group of **E1** and the phenyl side arm of the ligand **L*17** compared with transition state **TS3-*R***, whereas such a steric repulsion was absent in transition state **TS4-*S***. Such steric repulsion increased the energy gap between **TS4-*S*** and **TS4-*R*** to 1.9 kcal mol^{-1}, which agreed with the enhanced e.e. obtained experimentally. Therefore, the enantioenhancement was mainly controlled by the steric effect between the phenyl group of **E1** and the phenyl side arm of **L*17**, indicating that the steric effect in the distant region away from the copper centre was important for controlling stereoselectivity. Overall, these experimental and computational results supported our initial proposal and provided insights into the effect of chiral ligands on the enantioselectivity of this reaction.

Conclusions

In summary, we successfully developed a general strategy for the Cu-catalysed enantioconvergent radical *O*-alkylation of diverse alcohols with racemic α-tertiary haloamides. The key to success is the development of anionic *N*,*N*,*N*-ligands with a rigid side arm that create coordinatively saturated Cu(III) intermediates with low steric congestion around metal centre. This design could not only accommodate bulky alcohols with weak nucleophilicity, but also provide steric repulsion to increase the enantio-differentiation, therefore exerting remarkable chemo- and enantioselectivity. This method establishes a flexible platform for the construction of structurally diverse and synthetically challenging enantioenriched hindered ethers, especially α,α′-trisubstituted α-stereogenic ones that have not been previously disclosed. More importantly, the catalytic stereodivergent process has been developed to access all of the possible stereoisomers of hindered dialkyl ethers with two stereocentres at will with high catalyst-controlled stereoselectivity. We expect that this strategy will inspire more efforts in the development of asymmetric alkylation reactions of sterically congested nucleophiles derived from readily available starting materials, which will ultimately benefit the synthetic community and related research areas.

Methods

Representative procedure for the synthesis of 1–63, 102–103 and 114–116

Under an argon atmosphere, an oven-dried resealable Schlenk tube equipped with a magnetic stir bar was charged with α-tertiary haloamide (0.20 mmol; 1.0 equiv.), Cu(OTf)·tol$_{1/2}$ (5.17 mg; 0.02 mmol; 10 mol%), **L*17** or (*R*,*R*)-**L*17** (13.92 mg; 0.03 mmol; 15 mol%) and K_3PO_4 (128.0 mg; 0.60 mmol; 3.0 equiv.). The Schlenk tube was fully evacuated and backfilled with argon five times. Then, tertiary alcohol (0.30 mmol; 1.5 equiv.) and anhydrous DCE (2.0 ml) were sequentially added to the mixture. The tube was sealed and the reaction mixture was stirred at −10 or −20 °C. Upon completion (monitored by thin-layer chromatography), the precipitate was filtered off and rinsed three times by CH_2Cl_2 (5.0 ml). The filtrate was evaporated and the residue was purified by column chromatography on silica gel to afford the desired product.

Representative procedure for the synthesis of 64–90, 94–101 and 110–113

Under an argon atmosphere, an oven-dried resealable Schlenk tube equipped with a magnetic stir bar was charged with α-tertiary haloamide (0.20 mmol; 1.0 equiv.), Cu(NTf$_2$)$_2$ (12.5 mg; 0.02 mmol; 10 mol%), **L*22** or (*R*,*R*)-**L*22** (14.4 mg; 0.03 mmol; 15 mol%) and K_3PO_4 (128.0 mg; 0.60 mmol; 3.0 equiv.). The Schlenk tube was fully evacuated and backfilled with argon five times. Then, primary or secondary alcohol (0.30 mmol; 1.5 equiv.) and anhydrous DCE (2.0 ml) were sequentially added to the mixture. The tube was sealed and the reaction mixture was stirred at −10 °C for 5 days. Upon completion (monitored by thin-layer chromatography), the precipitate was filtered off and rinsed three

times by CH_2Cl_2 (5.0 ml). The filtrate was evaporated and the residue was purified by column chromatography on silica gel to afford the desired product.

Data availability

Data relating to the materials and methods, optimization studies, experimental procedures, mechanistic studies, DFT calculations, high-performance liquid chromatography spectra, NMR spectra and mass spectrometry data are available in the Supplementary Information. Crystallographic data for compounds **30**, **56**, **64**, **81** and **C2** are available free of charge from the Cambridge Crystallographic Data Centre under reference numbers CCDC 2386430 (for **30**), 2386428 (for **56**), 2386427 (for **64**), 2386429 (for **81**) and 2386426 (for **C2**). All of the other data are available from the authors upon reasonable request.

References

1. Roughley, S. D. & Jordan, A. M. The medicinal chemist's toolbox: an analysis of reactions used in the pursuit of drug candidates. *J. Med. Chem.* **54**, 3451–3479 (2011).
2. Flick, A. C. et al. Synthetic approaches to the new drugs approved during 2020. *J. Med. Chem.* **65**, 9607–9661 (2022).
3. Ameen, D. & Snape, T. J. Chiral 1,1-diaryl compounds as important pharmacophores. *Med. Chem. Commun.* **4**, 893–907 (2013).
4. María, P. D. D., Gemert, R. W. V., Straathof, A. J. J. & Hanefeld, U. Biosynthesis of ethers: unusual or common natural events? *Nat. Prod. Rep.* **27**, 370–392 (2010).
5. Carroll, A. R., Copp, B. R., Davis, R. A., Keyzers, R. A. & Prinsep, M. R. Marine natural products. *Nat. Prod. Rep.* **37**, 175–223 (2020).
6. Aiba, Y. et al. Total synthesis and antifungal activity of 9-methoxystrobilurin L as the originally proposed 1,4-benzodioxan structure. *Bioorg. Med. Chem. Lett.* **11**, 2783–2786 (2001).
7. Patel, A. V. et al. T-cadinol nerolidol ether from *Schisandra chinensis*. *Nat. Prod. Commun.* **3**, 1453–1456 (2008).
8. Shennan, B. D. A. et al. Branching out: redox strategies towards the synthesis of acyclic α-tertiary ethers. *Chem. Soc. Rev.* **51**, 5878–5929 (2022).
9. Shu, Y.-Z. Recent natural products based drug development: a pharmaceutical industry perspective. *J. Nat. Prod.* **61**, 1053–1071 (1998).
10. Martino, G. D. et al. Novel 1-[2-(diarylmethoxy)ethyl]-2-methyl-5-nitroimidazoles as HIV-1 non-nucleoside reverse transcriptase inhibitors. A structure–activity relationship investigation. *J. Med. Chem.* **48**, 4378–4388 (2005).
11. Kennemur, J. L., Maji, R., Scharf, M. J. & List, B. Catalytic asymmetric hydroalkoxylation of C–C multiple bonds. *Chem. Rev.* **121**, 14649–14681 (2021).
12. Cheng, Q. et al. Iridium-catalyzed asymmetric allylic substitution reactions. *Chem. Rev.* **119**, 1855–1969 (2019).
13. Pàmies, O. et al. Recent advances in enantioselective Pd-catalyzed allylic substitution: from design to applications. *Chem. Rev.* **121**, 4373–4505 (2021).
14. Zhu, S.-F. & Zhou, Q.-L. Transition-metal-catalyzed enantioselective heteroatom–hydrogen bond insertion reactions. *Acc. Chem. Res.* **45**, 1365–1377 (2012).
15. Guo, X. & Hu, W. Novel multicomponent reactions via trapping of protic onium ylides with electrophiles. *Acc. Chem. Res.* **46**, 2427–2440 (2013).
16. Wang, P.-Z., Chen, J.-R. & Xiao, W.-J. Emerging trends in copper-promoted radical-involved C–O bond formations. *J. Am. Chem. Soc.* **145**, 17527–17550 (2023).
17. Chang, R., Cai, S., Yang, G., Yan, X. & Huang, H. Asymmetric aminomethylative etherification of conjugated dienes with aliphatic alcohols facilitated by hydrogen bonding. *J. Am. Chem. Soc.* **143**, 12467–12472 (2021).
18. Liao, L., Xu, X., Ji, J. & Zhao, X. Asymmetric intermolecular iodinative difunctionalization of allylic sulfonamides enabled by organosulfide catalysis: modular entry to iodinated chiral molecules. *J. Am. Chem. Soc.* **144**, 16490–16501 (2022).
19. Yang, S.-Q. et al. Catalytic asymmetric hydroalkoxylation and formal hydration and hydroaminoxylation of conjugated dienes. *J. Am. Chem. Soc.* **145**, 3915–3925 (2023).
20. Li, Q., Wang, Z., Dong, V. M. & Yang, X.-H. Enantioselective hydroalkoxylation of 1,3-dienes via Ni-catalysis. *J. Am. Chem. Soc.* **145**, 3909–3914 (2023).
21. Zhang, G. et al. Asymmetric coupling of carbon-centered radicals adjacent to nitrogen: copper-catalyzed cyanation and etherification of enamides. *Angew. Chem. Int. Ed.* **59**, 20439–20444 (2020).
22. Li, R.-Z., Liu, D.-Q. & Niu, D. Asymmetric *O*-propargylation of secondary aliphatic alcohols. *Nat. Catal.* **3**, 672–680 (2020).
23. Nakajima, K., Shibata, M. & Nishibayashi, Y. Copper-catalyzed enantioselective propargylic etherification of propargylic esters with alcohols. *J. Am. Chem. Soc.* **137**, 2472–2475 (2015).
24. Zhu, S.-F., Cai, Y., Mao, H.-X., Xie, J.-H. & Zhou, Q.-L. Enantioselective iron-catalysed O–H bond insertions. *Nat. Chem.* **2**, 546–551 (2010).
25. Kang, Q.-K., Wang, L., Liu, Q.-J., Li, J.-F. & Tang, Y. Asymmetric H_2O-nucleophilic ring opening of D–A cyclopropanes: catalyst serves as a source of water. *J. Am. Chem. Soc.* **137**, 14594–14597 (2015).
26. Xia, Y. et al. Asymmetric ring-opening of cyclopropyl ketones with thiol, alcohol, and carboxylic acid nucleophiles catalyzed by a chiral *N*,*N*′-dioxide–scandium(III) complex. *Angew. Chem. Int. Ed.* **54**, 13748–13752 (2015).
27. Lai, Z., Wang, Z. & Sun, J. Organocatalytic asymmetric nucleophilic addition to *o*-quinone methides by alcohols. *Org. Lett.* **17**, 6058–6061 (2015).
28. Wang, J.-W. et al. Nickel-catalyzed remote asymmetric hydroalkylation of alkenyl ethers to access ethers of chiral dialkyl carbinols. *J. Am. Chem. Soc.* **145**, 10411–10421 (2023).
29. Ziegler, D. T. & Fu, G. C. Catalytic enantioselective carbon–oxygen bond formation: phosphine-catalyzed synthesis of benzylic ethers via the oxidation of benzylic C–H bonds. *J. Am. Chem. Soc.* **138**, 12069–12072 (2016).
30. Maier, T. C. & Fu, G. C. Catalytic enantioselective O–H insertion reactions. *J. Am. Chem. Soc.* **128**, 4594–4595 (2006).
31. Lamhauge, J. N., Corti, V., Liu, Y. & Jørgensen, K. A. Enantioselective α-etherification of branched aldehydes via an oxidative umpolung strategy. *Angew. Chem. Int. Ed.* **60**, 18728–18733 (2021).
32. Lin, Q. et al. Enantioselective S_N1-type reaction via electrochemically generated chiral α-imino carbocation intermediate. *Nat. Commun.* **15**, 6900 (2024).
33. Xiang, J. et al. Hindered dialkyl ether synthesis with electrogenerated carbocations. *Nature* **573**, 398–402 (2019).
34. Zhou, Z., Behnke, N. E. & Kürti, L. Copper-catalyzed synthesis of hindered ethers from α-bromo carbonyl compounds. *Org. Lett.* **20**, 5452–5456 (2018).
35. Hirata, G. et al. Chemistry of tertiary carbon center in the formation of congested C–O ether bonds. *Angew. Chem. Int. Ed.* **60**, 4329–4334 (2021).
36. Chen, X., Patel, K. & Marek, I. Stereoselective construction of tertiary homoallyl alcohols and ethers by nucleophilic substitution at quaternary carbon stereocenters. *Angew. Chem. Int. Ed.* **62**, e202212425 (2023).
37. Wu, F., Chang, J. & Bai, D. Synthesis of sterically hindered dialkyl ethers via palladium-catalyzed fluoro-alkoxylation of *gem*-difluoroalkenes. *Org. Lett.* **26**, 4953–4957 (2024).

38. Kumara, M. N., Nakahara, T., Kobayashi, S., Fujio, M. & Mishima, M. Nucleophilicities of alcohols and water in acetonitrile based on reactivities of benzhydrylium ions. *Bull. Chem. Soc. Jpn* **91**, 523–530 (2018).
39. Bordwell, F. G. Equilibrium acidities in dimethyl sulfoxide solution. *Acc. Chem. Res.* **21**, 456–463 (1988).
40. Williamson, A. Theory of etherification. *Philos. Mag.* **37**, 350–356 (1850).
41. Kürti, L. & Czakó, B. Strategic applications of named reactions in organic synthesis, 484–485 (Elsevier, 2005).
42. Schneider, N., Lowe, D. M., Sayle, R. A., Tarselli, M. A. & Landrum, G. A. Big data from pharmaceutical patents: a computational analysis of medicinal chemists' bread and butter. *J. Med. Chem.* **59**, 4385–4402 (2016).
43. Chen, C. & Fu, G. C. Copper-catalysed enantioconvergent alkylation of oxygen nucleophiles. *Nature* **618**, 301–307 (2023).
44. Chen, J.-J. et al. Enantioconvergent Cu-catalysed *N*-alkylation of aliphatic amines. *Nature* **618**, 294–300 (2023).
45. Du, X.-Y. et al. Copper-catalyzed enantioconvergent radical *N*-alkylation of diverse (hetero)aromatic amines. *J. Am. Chem. Soc.* **146**, 9444–9454 (2024).
46. Frisch, A. C. & Beller, M. Catalysts for cross-coupling reactions with non-activated alkyl halides. *Angew. Chem. Int. Ed.* **44**, 674–688 (2005).
47. Shibutani, S. et al. Organophotoredox-catalyzed decarboxylative C(sp^3)–O bond formation. *J. Am. Chem. Soc.* **142**, 1211–1216 (2020).
48. Crabtree, R. H. (eds) *The Organometallic Chemistry of the Transition Metals* (Wiley, 2006).
49. Wang, F.-L. et al. Mechanism-based ligand design for copper-catalysed enantioconvergent C(sp^3)-C(sp) cross coupling of tertiary electrophiles with alkynes. *Nat. Chem.* **14**, 949–957 (2022).
50. McGrath, N. A., Brichacek, M. & Njardarson, J. T. A graphical journey of innovative organic architectures that have improved our lives. *J. Chem. Educ.* **87**, 1348–1349 (2011).
51. Beletskaya, I. P., Nájera, C. & Yus, M. Stereodivergent catalysis. *Chem. Rev.* **118**, 5080–5200 (2018).
52. Krautwald, S. & Carreira, E. M. Stereodivergence in asymmetric catalysis. *J. Am. Chem. Soc.* **139**, 5627–5639 (2017).

Acknowledgements

Financial support from the National Natural Science Foundation of China (22025103, 22331006, 92256301 and 22401136), National Key R&D Program of China (2021YFF0701604 and 2021YFF0701704), Guangdong Innovative Program (2019BT02Y335), Guangdong Major Project of Basic and Applied Basic Research (2023B0303000020), Guangdong Basic and Applied Basic Research Foundation (2023A1515140088 and 2024A1515010325), Guangdong Provincial Key Laboratory of Mathematical and Neural Dynamical Systems (2024B1212010004), Guangdong Youth Scholars Program (2023TQ07A015), Shenzhen Science and Technology Program (KQTD20210811090112004, JCYJ20220818100600001 and JCYJ20240813094223031), Shenzhen Key Laboratory of Cross-Coupling Reactions (ZDSYS20220328104200001) and New Cornerstone Science Foundation through the XPLORER PRIZE is gratefully acknowledged. We appreciate the assistance of SUSTech Core Research Facilities. Computational work was supported by the Center for Computational Science and Engineering and the CHEM High-Performance Supercomputer Cluster of the Department of Chemistry, Southern University of Science and Technology.

Author contributions

J.-Y.Z. and J.-J.C. designed the experiments and analysed the data. J.-Y.Z., J.-J.C., J.-H.F., X.-Y.D., N.-Y.Y., C.-J.Y., W.-L.L., F.L. and Z.D. performed the experiments. P.Y. designed the DFT calculations. B.S. performed the DFT calculations. Z.-L.L., Q.-S.G. and X.-Y.L. wrote the manuscript. X.-Y.L. conceived of and supervised the project.

Competing interests

The authors declare no competing interests.

Additional information

Supplementary information The online version contains supplementary material available at https://doi.org/10.1038/s41929-025-01402-w.

Correspondence and requests for materials should be addressed to Peiyuan Yu or Xin-Yuan Liu.

Peer review information *Nature Catalysis* thanks the anonymous reviewers for their contribution to the peer review of this work.

Reprints and permissions information is available at www.nature.com/reprints.

Publisher's note Springer Nature remains neutral with regard to jurisdictional claims in published maps and institutional affiliations.

[1]Shenzhen Key Laboratory of Cross-Coupling Reactions, Southern University of Science and Technology, Shenzhen, China. [2]Shenzhen Grubbs Institute, Department of Chemistry and Guangming Advanced Research Institute, Southern University of Science and Technology, Shenzhen, China. [3]Department of Chemistry, Great Bay Institute for Advanced Study and Guangdong Provincial Key Laboratory of Mathematical and Neural Dynamical Systems, Great Bay University, Dongguan, China. [4]Dongguan Key Laboratory of Interdisciplinary Science for Advanced Materials and Large-Scale Scientific Facilities, School of Physical Sciences, Great Bay University, Dongguan, China. [5]These authors contributed equally: Jia-Yong Zhang, Ji-Jun Chen, Boming Shen. ✉e-mail: yupy@sustech.edu.cn; liuxy3@sustech.edu.cn